Selective Precipitation of Value-Nonferrous Metals Components from the Slags

Zhitong Sui Nianxin Fu Peixin Zhang

Dept.of Nonferrous Metallurgy
Northeastern University
Shenyang 110006,P.R.China,
Phone Number 86-024-3893000-7731

ABSTRACT

The selective precipitation of B and/or Ti components was summarized, as examples of the precipitating selectivity of value-nonferrous metals components (VNMC) from the slags. It was confirmed that the recovery efficiency of VNMC (REVNMC) was depended on proper precipitating feature of VNMC in the slags. The optimum operation factors were discussed in order to approach the selective precipitation of VNMC from the slags and to fulfill the goal of efficient recovery. The precipitating mechanism was investigated by the way of mainly TEM observation in situ of heating sample and then the computer simulation combined with fractal description as auxiliary.

1. INTRODUCTION

China bounds in mineral resources of iron, but the some of that are composite mineral ores containing value-nonferrous metals components (VNMC), such as Ludwigite Deposited in Dandong, V-Ti-bearing magnetite in Penzhihua and RE-bearing ore in Baotou (Table I).

Due to complex mineralogy, very fine mineral dissemination and low grade, firstly, the key technique to exploit and utilize the ore lies on the separating the nonferrous metals and iron availably.

When the ores were usually treated in a blast-furnace, the nonferrous metal oxides were mostly concentrated in molten slags and separated from liquid pig-iron. So blast-furnace slags become an important man-made resources (Table II). Hence secondly the urgent need is to recovery VNMC from the slags efficiently.

It was indicated by a series of experiments that the recovery efficiency of value-nonferrous metals component (REVNMC) from the slags was directly related to the characteristics of VNMC bearing the slags, such as occurrences, morphology, grain size and distribution etc. For instance, when the molten B-slags were quickly cooled and then the most of boron component existed in the form of amorphous phase, the recovery efficiency of boron (REB) was low . While the REB was high when the slags were slowly cooled down and then the boron components existed in the form of crystallized phase.

The situation was similar to the slags containing titanium which was existed in the form of different mineral components like perovskite ($CaO \cdot TiO_2$), titanaugite m ($CaO \cdot MgO \cdot 2 SiO_2$) n [$CaO (Al \cdot Ti)_2 O_3 \cdot SiO_2$] and rich-titanium diopside etc. These mineral components showed the poor liberation, very fine and dispersed grain, so the recovery efficiency of titanium (RET) was low. However, higher RET was availably reached after the suitable addition and heat-treatment on the slags.

Obviously, the essence to increase REVNMC is to control artificially the precipitating characteristics of VNMC during the slags cooling process. In other words, the selective precipitation of VNMC is common and crucible problems for recovering process designed.

The present paper is the summary of the study works on the selective precipitation of boron and/or titanium bearing slags through two aspects: the precipitating behavior of B and/or Ti and the factors affecting the REVNMC, since the optimization of the recovering process must arise from a fundamental understanding of the process involved.

Table I Composition of iron ore(wt.%)

Ore	TFe	CaO	SiO_2	Al_2O_3	MgO	B_2O_3	TiO_2	V_2O_5	REO	F	Nb_2O_5
Ludwigite	30	0.4	15	1.5	24	7	0	0	0	-	-
V-Ti magnetite	33.40	5.82	18.42	9.18	5.0	0	11.45	0.33	0	-	-
RE-bearing ore	48	8.78	4.81	0.22	1.0	0	0.29	0	2.73	5.89	0.06

Table II Composition of blast-furnace slags (wt.%)

Slag	CaO	SiO_2	Al_2O_3	MgO	B_2O_3	TiO_2	V_2O_5	REO	F
B-slag	5-10	5-35	5-10	35-45	12-15	0	0	0	0
Ti-slag	27-28	22-25	14-15	7-8	0	23-25	0.32	-	-
RE-slag	37-43	20-25	-	-	0	0	0	10-18	8-11

2. PRECIPITATION BEHAVIOR AND CHARACTERISTICS OF VNMC IN COOLING PROCESS

The technique of TEM observation in situ heating sample is an available method for studying the precipitation behavior and characteristics of VNMC during the solidification of molten slags, but the computer simulation combined with fractal description is also an auxiliary means to reveal the precipitation mechanism and to understand the precipitation process further.

2.1 Precipitation behavior of boron components in slags

2.1.1 Precipitation characteristics [1]

The consequences of TEM observation in situ of heating samples showed that the precipitating process involved two steps: the phase separation of amorphous phases and the crystal precipitation. When temperature was raised at 400 ℃, some more isolated drop shaped amorphous phases firstly appeared on the matrix of sample and then they gradually grew up to be in connective form in Fig.1a. Around 700 ℃ a few of crystalline phases were precipitated on the base of the amorphous phases and then at 900 ℃ they were grown up as the Suanite ($2MgO \cdot B_2O_3$) dendrite which was confirmed by electron diffraction analysis in Fig.1b.

2.1.2 Computer simulation combined with fractal description [2]

Usually it is difficult to reveal precipitating mechanism just by micrographs which fortunately show fractal character. Consequently the mechanism could be studied by the computer simulation combined with fractal description. The fractal dimension of the amorphous phases at the phase separation step (in Fig.1a) was determined to be in range of 1.87-1.92 by area-radius gyration. On the other hand, the fractal dimension of the picture of hypothetical phase separation simulated by Monte-Carlo method based on the Spinodal decomposition model was calculated to be 1.91 in Fig.2a.

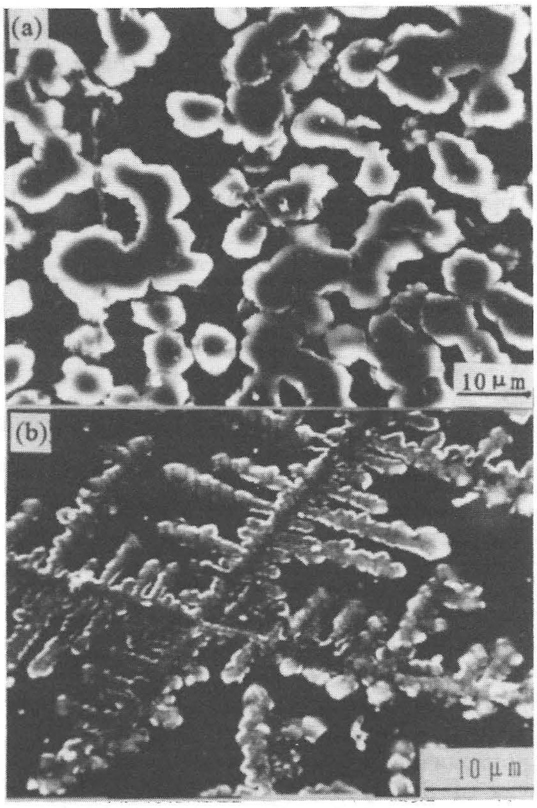

Fig.1. TEM micrographs of the samples at 400 ℃ and 900 ℃ (a) 400 ℃, (b) 900 ℃

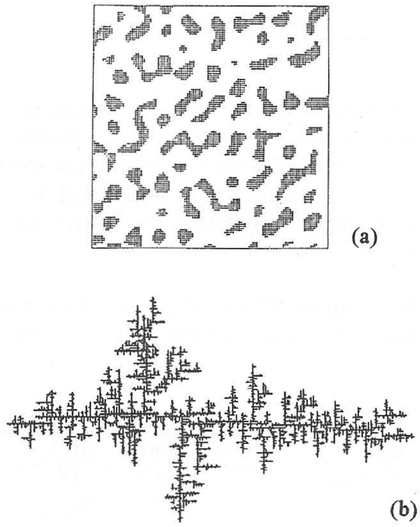

Fig.2 Results of computer simulation for (a)phase separation (b) the Suanite growth

It is indicated by comparison with the fractal dimension and the micrographs of both experiments and simulations that mechanism of the phase separation is confirmed in conformity to the Spinodal decomposition model. Following the same procedure, the fractal dimension of the Suanite's dendrite at 900 ℃ was 1.63 (Fig.1b), but that of the dendrite, which was simulated based on the DLA(Diffusion Limited Aggregation) model, was 1.62 in Fig.2b. Therefore, the crystal growth for the Suanite is dependent on the DLA model.

2.2 Precipitation behavior of titanium components in slags

2.2.1 Precipitation process of the Perovskite phase

Molten Ti-slag was treated at temperature of 1400 ℃ with holding times of 30 min, 60 min, 120 min, respectively, and then was quenched in water for investigation. It was indicated that the Perovskite phase was firstly precipitated in the form of fine and isolated dendrites with primary arms and secondary arms in Fig.3a, holding 30 min, and then some secondary arms were in contact with each other and were coarsened after 60 or 120 min in Fig.3b. It was indicated by observing the microstructures that the larger secondary arms were grown at the expense of the smaller ones as the number of them were decreased to maintain a constant volume fraction of precipitation.

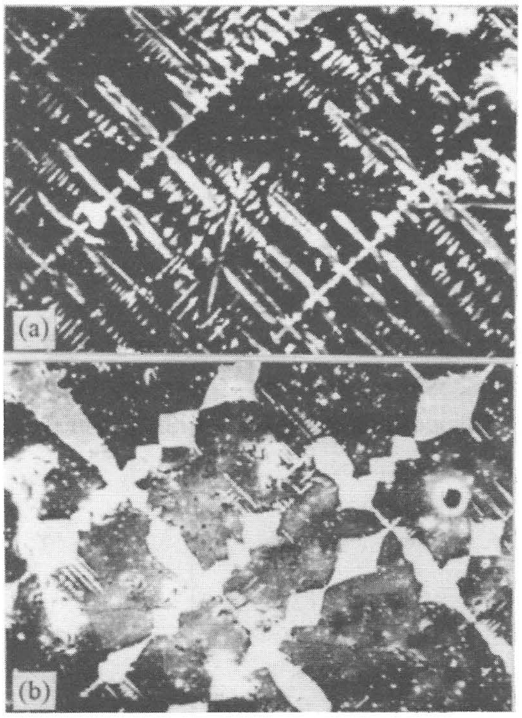

Fig.3 SEM micrographs of sample treated at 1400 ℃(a) for 30 min,(b) for 120 min

The grain size of the Perovskite phase was increased continuously with time at 1350 ℃, in Fig.4a. based on which the curve of $\bar{d}^3$ against time was drawn in Fig.4b. It was seen that the points approximately lie along straight line which indicates that the grain growth was controlled by diffusion, so the equation can be written[3]:

$$\bar{d}^3 - \bar{d}_0^{\,3} = kt \qquad (1)$$

Where $\bar{d}$ is mean grain size at time t, $\bar{d}_0$ is at time t =0, and k is a rate constant which is determined to be 0.244 × 10^4 $\mu m^3/h$. Therefore, the growth of the Perovskite phase may obey Ostwald ripening [4,5] during the coarsening process whose driving force was the reduction in the free energy associated with the decreasing surface area.

2.2.2 Computer simulation of the Perovskite crystals growth [6]

The growth process of crystals was simulated based on the modified DLA model. A particle representing a initial nucleus was positioned in the center of screen, and then other particles were moved toward the nucleus randomly. The particle clusters were formed as the particles were encountered with the nucleus. When the

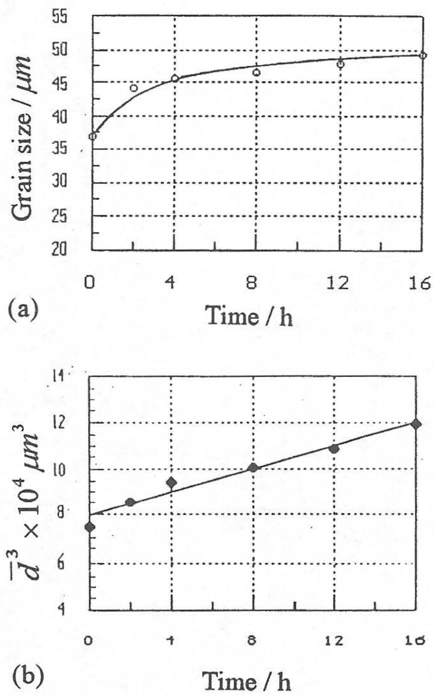

Fig.4 (a) The growth of the Perovskite phase with time,(b)Plot of $\bar{d}^3$ against time growth rate at the tip of particle clusters was about twice as large as that at the broadside, the particle clusters were grown in the form of fine and long dendrites with primary arms and secondary arms, which became elongated with increasing particles, in Fig.5(a). When the growth rates at the tip and the broadside were close, the particle clusters were grown in the form of thick and short dendrites which were coarsened into equiaxed grains in Fig.5(b) due to mergers of the secondary arms. Comparing the experimental results with these simulated ones, it can be found that the Perovskite morphology in Fig.6(a) obtained by cooling rate of 2 ℃/min from 1400 ℃ to 1200 ℃ was similar to the fine dendrites in Fig.5(a), and that obtained by cooling rate of 0.5 ℃/min in Fig.6(b) was similar to the coarsening equiaxed grains in Fig.5(b).

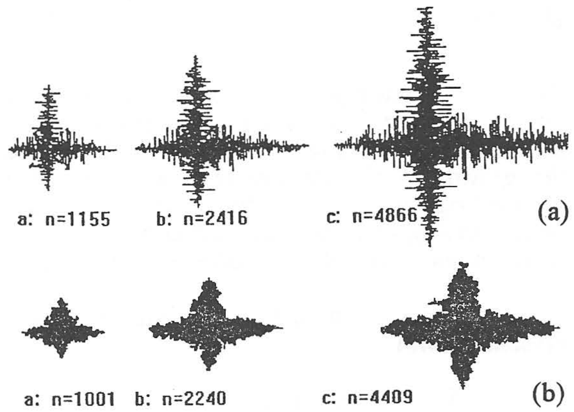

Fig.5 Computer simulation for perovskite (a)dendrites, (b) equiaxed rains.

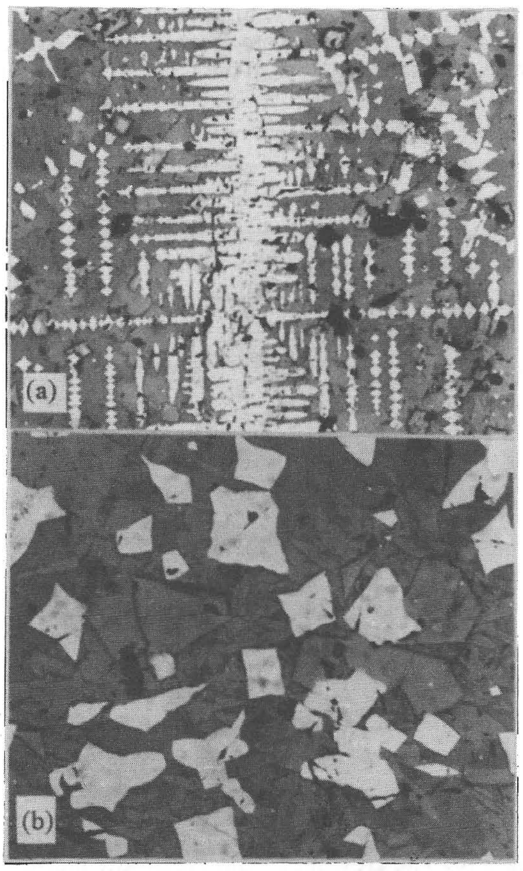

Fig.6 Micrographs of the Perovskite phase at cooling rate of (a) 2 ℃/min,(b) 0.5 ℃/min

3. FACTORS AFFECTING SELECTIVE PRECIPITATION

The study on the factors affecting precipitation behavior of VNMC in slags and their quantization relations is an aid to artificially control the precipitation morphology and characteristics so as to realize the purpose of selective precipitation.

3.1 Chemical composition

3.1.1 Optimization of B-slags composition by Artificial Neural Networks

The relationship between the REB and composition was investigated. The composition of samples selected was shown in Fig.7 in which the composition of the samples having high REB was just located along the line between the Suanite and the Forsterite($2MgO \cdot SiO_2$). The farther the composition deviated from the line, the lower the REB was [1].

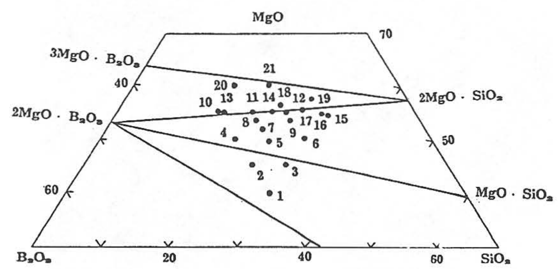

Fig.7 Composition of $MgO-B_2O_3-SiO_2$ system

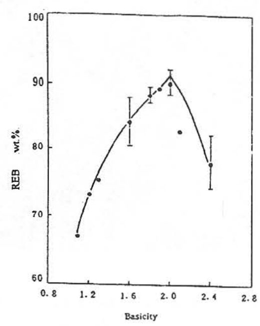

Fig.8 Variation of REB with basicity

The relationship between the REB and the basicity [$R = MgO / (B_2O_3 + SiO_2)$] was also investigated in Fig.8, which showed that the compositions for R=2.0 were just located along the line, so the REB were the highest.

By Artificial Neural Network(ANN), the relation between the composition and the REB has been modeled [7]. A 3 × 2 × 1 three layered feed-forward neural network was used for modeling in this paper, as showed in Fig.9. The input elements Z_1, Z_2 and Z_3 represent the percentages of MgO, SiO_2 and B_2O_3, respectively. Y_j (j=1,2) represent the outputs of the hidden neurons. The output of the

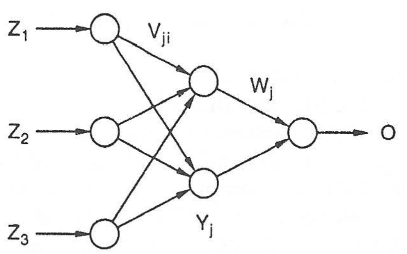

Fig.9 Back-propagation structure of artificial neural of network

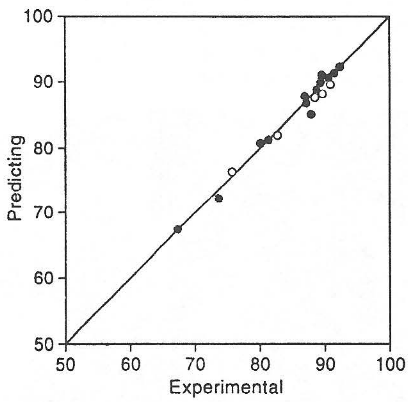

Fig.10 Results of artificial neural of network training and predication
● training, O predicated

networks O,will approximate the REB. The symbol $V_{j,i}$ represents the connection weights between the *i*th neuron of the input layer and the *j*th neuron in the hidden layer. W_j , the connection weight between the *j*th neuron in the hidden layer and the output neuron. Sixteen samples from twenty-one were randomly selected for training the ANN. The remaining five samples were used to verify the generalization capability of the ANN. The REB of twenty-one samples was showed in Fig.10. The predicted REB, O, of the ANN were very close to experimental REB, O, not only for the training samples but also for the verifying samples. Maximal relative error is 3.3% but within 1.5% for the most samples. The optimum composition has been predicated by genetic algorithm to be 54% MgO, 11% B_2O_3, 35% SiO_2 which is just on the line between the Suanite and the Forsterite (in Fig.7).

3.1.2 Optimization of Ti-slags composition

The simple ternary system $CaO-SiO_2-TiO_2$ was chosen due to smaller contents of MgO and Al_2O_3 in the slag. The amount of the Perovskite phase was determined by orthogonal designs under the same cooling conditions, i.e. isothermal annealing for 2 h at 1400 ℃. The experimental results indicated that the amount of the Perovskite phase was increased with increasing the basicity (CaO/SiO_2) at fixed content of CaO and/or with increasing the content of CaO at fixed basicity. Meanwhile, the morphology of the Perovskite phase was also changed from dendrites to equiaxed crystals. Optimized condition for producing the Perovskite phase was the basicity of 1.4, 30%CaO and 26%TiO_2. The amount of the Perovskite phase was 22.57% on this condition.

3.2 Temperature of heat treatment [8]

During the cooling process, precipitation of VNMC in molten slags was dependent on nucleation rate I and crystal growth rate U, which are a function of temperature. According to the crystallization kinetics, the respective rates can be expressed as following equations:

$$I = \frac{N_0 kT}{3\pi\alpha^3\eta}\exp\left(-b\frac{\alpha^3\beta}{(\Delta Tr)^2 Tr}\right) \quad (2)$$

$$U = \frac{fkT}{3\pi\alpha^2\eta}\left[1-\exp\left(-\frac{\beta\Delta Tr}{Tr}\right)\right] \quad (3)$$

Usually, the optimum temperature corresponding to the highest nucleation rate I was not consistent with that corresponding to the highest crystal growth rate U. When the temperature was in range of 1100 ~ 1200 ℃, both I and U can approach to higher values simultaneously for the Suanite phase (in Fig.11). The most powerful crystallization occurred at 1100 ℃ which, of course, was the optimum temperature for heat treatment. Experimental results of the REB at different temperatures and the XRD at 1100 ℃ were showed

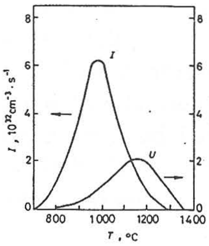

Fig.11 Effect of temperature on rates of I and U of the Suanite crystal

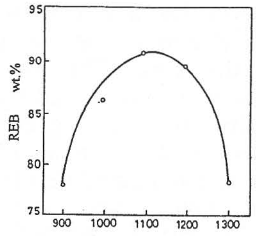

Fig.12 Variation of REB with temperature of heat treatment

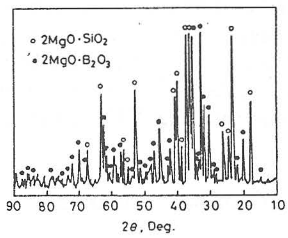

Fig.13 XRD pattern of the slag treated at 1100 ℃

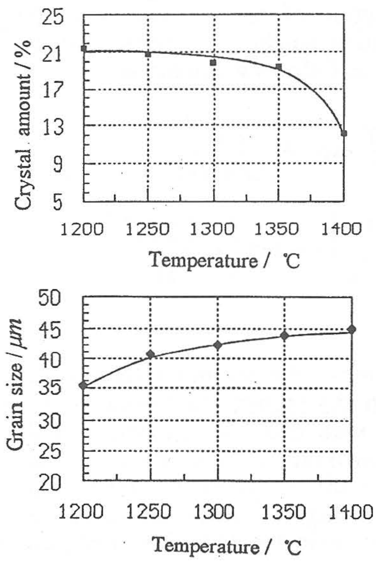

Fig.14 The plot of the amount and the grain size vs. temperature in isothermal process

in Fig.12 and Fig.13, respectively. The optimum temperature calculated by the equations is in good agree with experimental results.

Similarly, both I and U for the Perovskite phase approached to higher values in range of 1250-1350 ℃, and the optimum temperature for heat treatment was 1350 ℃, which agrees with the experimental results about the amount and the grain size of the Provskite phase in Fig.14 .

3.3 Additive agents

Additive agents are also a factor affecting the precipitation behavior of VNMC, besides chemical composition and heat treatment.

3.3.1 Effects of additive agents on precipitation behavior of the Suanite phase [9]

The microstructure of sample 1 without any additive agent was showed in Fig.15. The most of the visual field in sample 1 were covered by amorphous phases (over 80%) in which a small amount of the Suanite phase were distributed. The addition of titania to sample 1 caused the reducing amorphous phase from 80% to 60% and the growing crystallites to cluster (Fig.16a), so that the REB was increased by 3 ~ 4%. Similarly, addition of MO_x to sample 1 facilitated the growing crystallites to large host grains with very little amorphous phases remained (Fig. 16b). As a result, the REB was increased by 8 ~ 11%.

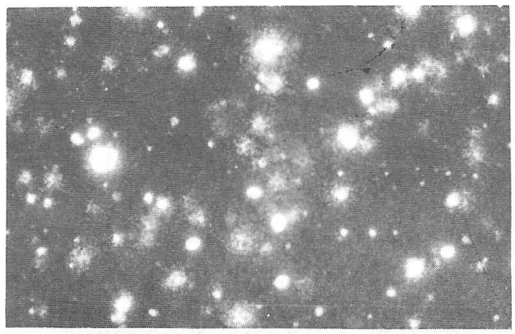

Fig.15 The micrographs of samples 1

The mechanism of effects of additive agents on micrographs and REB can be studied further. The chemical composition of sample 22 was 45%MgO, 20% B_2O_3, 35%SiO_2, which was added by 2% TiO_2 as sample 23 and 2% MO_x as sample 24, respectively. The activation energy of crystallization has been calculated by Kiss-inger equation [10-12]

$$\ln\left(\frac{T_P^2}{\varphi}\right) = \frac{E}{RT_P} + \text{Const.} \qquad (4)$$

where E is activation energy of crystallization, T_p temperature of crystallization, φ heating rate.

A plot of $\ln\left(T_P^2 / \varphi\right)$ vs. $1/T_p$ should be a straight line, from which E can be determined by the slope. Values of activation energy of crystallization were calculated using Eq.(4), as E_{22} = 484kJ/mol, E_{23} = 421kJ/mol, E_{24} = 409kJ/mol. It was indicated that the activation energies of crystallization were remarkably decreased by addition of TiO_2 and MO_x. Obviously, the addition can promote the precipitating of the crystalline phases and then improve the REB.

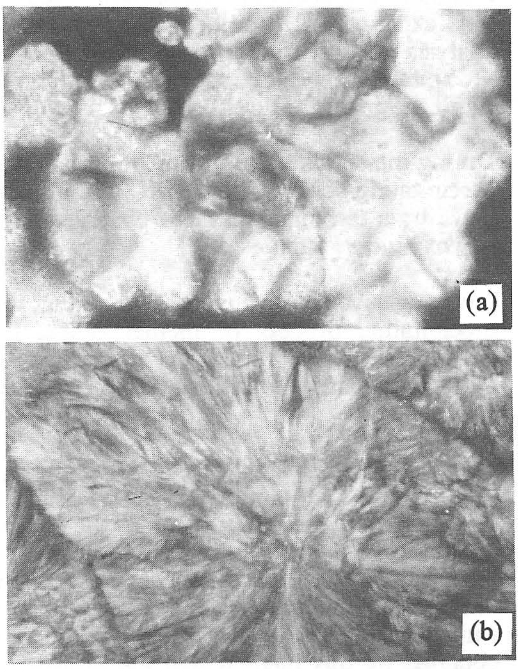

Fig.16 The micrographs of sample 1 with 3% (a)TiO_2 and (b)MO_x

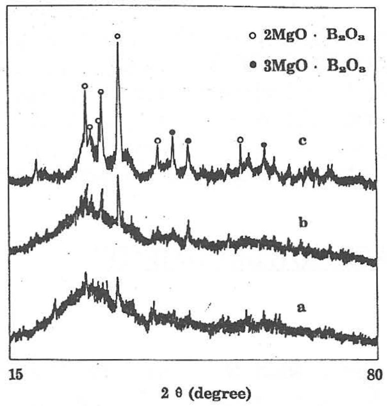

Fig.17.XRD patterns of samples,a-sample 22, b-sample 23, c-sample 24

The XRD patterns of samples annealed at 750 ℃ for 1h and heated at 850 ℃ for 30min were shown in Fig.17, which reveal that the host crystalline phase was the Suanite and the minor crystalline phase was 3MgO · B_2O_3, but the amount of crystalline phase in sample 24 was more than that in sample 23. Obviously, addition of MO_x improves the borates to precipitate in the form of the Suanite and 3MgO · B_2O_3.

The IR results showed that three weak peaks were found in the wave numbers of 490cm^{-1}, 533cm^{-1} and 930cm^{-1} because of addition of TiO_2 in Fig.18. They belong to the characteristic vibration of [B_2O_5] [13], the curve vibrations of [BO_3] take place in the range between 540-590cm^{-1}, the symmetry expand and contract of [BO_3] appear in the range between 900-950cm^{-1}, and the non symmetry expand and contract of [BO_3] occur in the range between 1000-1260cm^{-1} [14]. It was suggested that there were a lot of [B_2O_5] and [BO_3] in the slag structures. From the viewpoint of crystal chemistry, the two structures are favorable to make the Suanite and 3MgO · B_2O_3 precipitate.

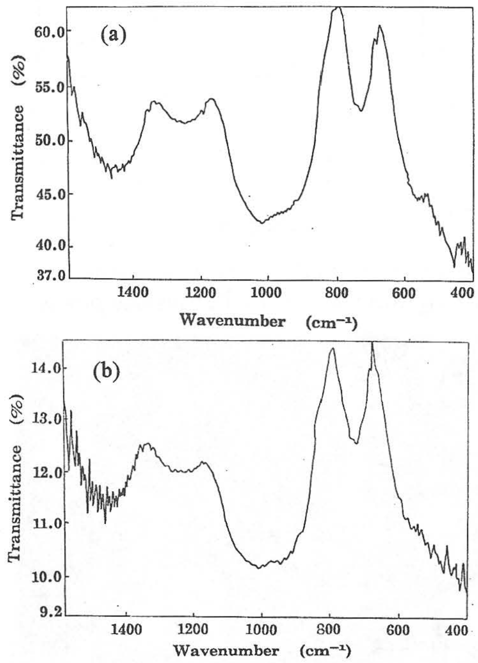

Fig.18 IR spectra of samples (a) sample 22, (b) sample 23

3.3.2 Effects of additive agents on preci-pitation behavior of the Perovskite phase [6]

The amount and the grain size of the Perovskite phase were increased efficiently by addition of Cr_2O_3, as shown in Fig.19.

Moreover, micrographs of the Perovskite phase were also changed from dendrites to equiaxed crystals by addition of 3% Cr_2O_3. The role of Cr_2O_3 was increasing the relative growth rate at the broadside of the Perovskite dendrites to match that at the tip of them. As a result, the secondary arms of dendrites were developed so that they were merged into equiaxed crystals (in Fig.20) which were beneficial to improve the RET.

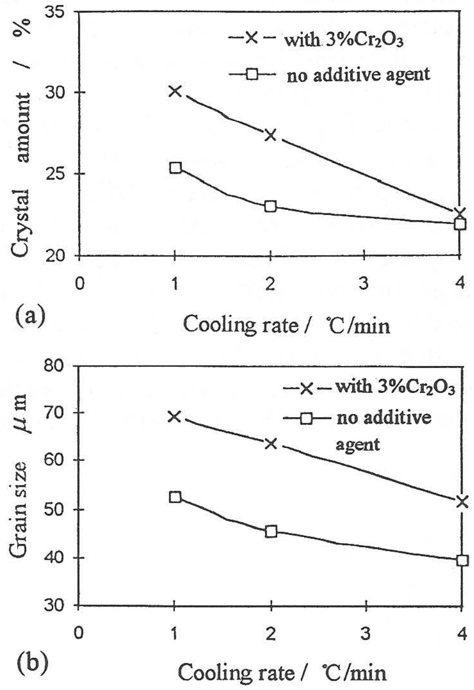

Fig.19.Effects of 3%Cr_2O_3 on (a)crystal amount,(b)grain size of the Perovskite phase

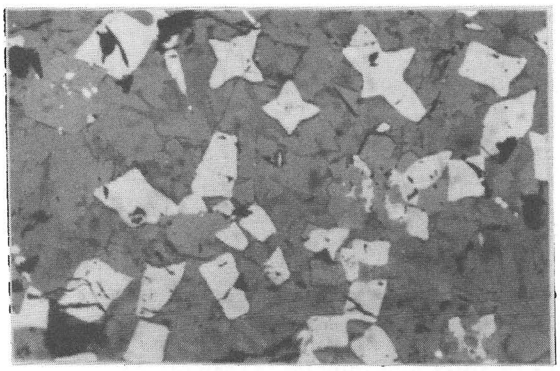

Fig.20. Micrographs of the Perovskite phase with 3%Cr_2O_3

4. CONCLUSION

(1) It was confirmed by experimental results of study on the precipitation of B and /or Ti from the slags that the REM was depended on proper precipitating feature of B and/or Ti components in the slags, such as morphology, structure, phase composition, crystallized state,grain size and dispersity, which were closely related to the operation factors like the slag composition, heat treatment temperature, cooling rate and additive agents.

Based on the optimum factors, the Boron components in the slag can be preferentially precipitated in the form of the Suanite and the Titanium in the Perovskite. As results the REM were increased obviously.

These facts may come to the conclusion that the precipitating behavior of VNMC from the slags could be artificially controlled by designing the operation conditions based on the experimental results and theoretical analysis so as to approach the selective precipitation of VNMC from the slags and to fulfill the goal of efficient recovery.

(2) During the solidification of molten slags, the precipitating behavior of VNMC was investigated by a technique of TEM observation in situ of heating sample.

It was discovered by the observation that the precipitating process of molten B-slag involved two steps: firstly the separation of amorphous phases and then the precipitation of the Suanite.

Usually, it is difficult to reveal a precipitating mechanism just by micrographs observation, but available method to study the precipitating mechanism is the way of mainly TEM observation in situ of heating sample and then the computer simulation combined with fractal description as auxiliary. It was obtained by this method that the growth of the Suanite and the Perovskite were depended on the DLA model and phase separation on the Spinodal decomposition.

(3) The investigation on the selective precipitation of B and/or Ti components is just examples by which both available research method and theoretical analysis model for studying on the precipitating selectivity of VNMC from the slags might be summarized.

ACKNOWLEDGMENT

The authors wish to thank "the Doctoral Foundation of State Education Commission of China" and "the National Natural Science Foundation of China" for financial support.

REFERENCES

1. P.X. Zhang, Z.T. Sui, " Effect of Factors on the Extraction of Boron from Slags " , Metall. Trans., Vol. 26B, 1995, pp.345-351.

2. P.X. Zhang , Z.T. Sui, " Computer simulation for fractal crystallization in $MgO\text{-}B_2O_3\text{-}SiO_2$ system " , J. of the Chinese Ceramic Society, Vol.23, 1995, pp.555-558.

3. Sung-Chul Yang, " Grain growth kinetics in liquid phase sintered zinc oxide-barium oxide ceramics " , J. Am. Ceram. Soc., Vol.74, No.12, 1991, pp.3085-90.

4. Thae-Khapp kang, " Coarsening of Tungsten Grains in Liquid Nickel-Tungsten Matrix " , Metall. Trans. , Vol.9A, Much, 1978, pp.433-438.

5. B.P.GU, " Coarsening of δ'(Al_3Li) precipitates in an Al-2.8Li-0.3Mn alloy " ,Materials Science and Engineering , Vol. 70, 1985, pp. 217-228.

6. Lu Ling, " Precipitating Behavior of Perovskite Phase in Titaniferous Slag " , Thesis of mater's degree, Northeastern University, 1996.

7. P.X. Zhang , Z.T. Sui, " Optimization of compositions of $MgO\text{-}B_2O_3\text{-}SiO_2$ slags using artificial neural networks and genetic algorithm ", Zeitschrift für Metallkunde, Vol.87, 1996, pp.76-78.

8. P.X. Zhang , Z.T. Sui, " Crystallization kinetics of the component containing boron in $MgO\text{-}B_2O_3\text{-}SiO_2\text{-}Al_2O_3\text{-}CaO$ slag " , Scandinavian Journal of Metallurgy, Vol.23, 1994, pp.244-247.

9. P.X. Zhang , Z.T. Sui, " Effects of nucleation agents on the crystallization behavior of boron contained in $MgO\text{-}B_2O_3\text{-}SiO_2$ slags ",The 2nd Int. Sym.on East Asian Resources Recycling Tech., Seoul, October 14-16, 1993, pp.403-411.

10. H.E.Kissinger, J.Res. Nat. Bur. Stand., Vol.57, 1956, pp.217.

11. H.E.Kissinger,Anal. Chem., Vol.29, 1957, pp.1702.

12. N.P.Bansal , R.H. Doremas, J.Thermal Anal., Vol.29, 1984, pp.115.

13. Peng Wenshi, G.K. Liu, Atlases of Infrared Ray of Mineral, Science Press, Beijing, China, 1982, 179.pp.1702.

14. Yong Nanru, The Testing Method of Material of Inorganic Non-Metal, Wuhan University of Technology Press, Wuhan, China, 1990, pp.273.

For further information on this paper, please contact professor Z.T.Sui at Shenyang, Liaoning province, P.R. China, 110006, P.O. Box 119, Fax (024) 3913669.